MPMI Vol. 26, No. 7, 2013, pp. 745–757. http://dx.doi.org/10.1094/MPMI-06-12-0154-R.

e-Xtra*

In Planta Effector Competition Assays Detect *Hyaloperonospora arabidopsidis* Effectors That Contribute to Virulence and Localize to Different Plant Subcellular Compartments

Jorge Luis Badel, Sophie J. M. Piquerez, David Greenshields, Ghanasyam Rallapalli, Georgina Fabro, Naveed Ishaque, and Jonathan D. G. Jones

The Sainsbury Laboratory, John Innes Centre, Norwich Research Park, Norwich, NR4 7UH, U.K.

Submitted 15 June 2012. Accepted 14 March 2013.

The genome of the pathogenic oomycete *Hyaloperonospora arabidopsidis* is predicted to encode at least 134 high-confidence effectors (HaRxL) carrying the RxLR motif implicated in their translocation into plant cells. However, only four avirulence genes (*ATR1*, *ATR13*, *ATR5*, and *ATR39*) have been isolated. This indicates that identification of HaRxL effectors based on avirulence is low throughput. We aimed at rapidly identifying *H. arabidopsidis* effectors that contribute to virulence by developing methods to detect and quantify multiple candidates in bacterial mixed infections using either Illumina sequencing or capillary electrophoresis. In these assays, referred to here as in planta effector competition assays, we estimate the contribution to virulence of individual effectors by calculating the abundance of each HaRxL in the bacterial population recovered from leaves 3 days after inoculation relative to abundance in the initial mixed inoculum. We identified HaRxL that enhance *Pseudomonas syringae* pv. *tomato* DC3000 growth in some but not all *Arabidopsis* accessions. Further analysis showed that HaRxLL464, HaRxL75, HaRxL22, HaRxLL441, and HaRxL89 suppress pathogen-associated molecular pattern-triggered immunity (PTI) and localize to different subcellular compartments in *Nicotiana benthamiana*, providing evidence for a multilayered suppression of PTI by pathogenic oomycetes and molecular probes for the dissection of PTI.

Plant pathogens have evolved sophisticated mechanisms to subvert the resistance response mounted by the plant immune system and to acquire nutrients. In the first layer of plant immunity, pattern recognition receptors recognize microbe-associated molecular patterns or pathogen-associated molecular patterns (PAMPs) (Jones and Dangl 2006; Zipfel and Robatzek 2010). This recognition triggers a response known as PAMP-triggered immunity (PTI) that is associated with changes in ion influx or efflux over the plasma membrane, generation of reactive oxygen species, deposition of callose, and induction of mitogen-activated protein kinase signaling cascades and defense-related genes (Jones and Dangl 2006; Zipfel and Robatzek 2010). Pathogens counteract PTI by delivering effector proteins that either block the recognition of PAMPs or target PTI downstream signaling components (Gohre and Robatzek 2008). Some effectors are recognized by a second layer of immunity conferred by intracellular resistance (R) proteins that perceive them (directly or indirectly), mounting a response known as effector-triggered immunity (ETI) that typically culminates in the hypersensitive response (HR) (Klement and Goodman 1967). Effectors recognized by cognate R proteins are often called avirulence proteins (Mansfield 2009). In response to ETI, pathogens have evolved effector proteins that either avoid recognition by R proteins or suppress the downstream signaling associated with ETI (Jones and Dangl 2006).

Hyaloperonospora arabidopsidis is an obligate biotrophic oomycete pathogen of *Arabidopsis* that causes downy mildew (Holub 2008). Only four *H. arabidopsidis* effector genes (*Arabidopsis thaliana* recognized [*ATR*]*1*, *ATR5*, *ATR13*, and *ATR39*) (Allen et al. 2004; Bailey et al. 2011; Goritschnig et al. 2012; Rehmany et al. 2005) have been cloned and confirmed as bona fide effectors because of their recognition by the cognate resistance genes. This low number emphasizes the necessity to undertake alternative approaches to identify and validate bona fide effectors. ATR1, ATR13, and ATR39 carry an RxLR (Arg, any amino acid, Leu, Arg) motif that is also present in effector genes from other oomycete plant pathogens such as *Phytophthora infestans* and *P. soja*e (Birch et al. 2006; Jiang et al. 2008). RxLR effectors are modular proteins characterized by an N-terminal signal peptide, an RxLR motif that has been implicated in translocation into the plant cell (Bhattacharjee et al. 2006; Dou et al. 2008b; Grouffaud et al. 2008; Whisson et al. 2007), and a C-terminal effector domain that is under positive selection (Win et al. 2007).

Genome analysis of *H. arabidopsidis* race Emoy2 revealed 134 high-confidence effector candidates (*HaRxL* genes) (Baxter et al. 2010). However, it is necessary to validate bioinformatics assessments experimentally. High-throughput screens for in planta effector function are therefore necessary to identify bona

Current address for J. L. Badel: Universidade Federal de Viçosa, BIOAGRO, Laboratorio de Genómica, Viçosa MG 36570-000, Brazil.

Current address for D. Greenshields: Novozymes BioAg Ltd., 3935 Thatcher Avenue Saskatoon, SK S7R 1A3, Canada.

Current address for G. Fabro: CIQUIBIC-CONICET, Departamento de Química Biológica, Facultad de Ciencias Químicas, Universidad Nacional de Córdoba, Córdoba, Argentina.

Corresponding author: D. G. Jones; Telephone: +44 (0) 1603 450 327; E-mail: jonathan.jones@sainsbury-laboratory.ac.uk

*The *e*-Xtra logo stands for "electronic extra" and indicates that eight supplementary figures and five supplementary tables are published online.

fide effectors from pools of HaRxL. Because methods for *H. arabidopsidis* transformation have not yet been developed, oomycete effector screens have been conducted with heterologous systems (Dou et al. 2008a; Oh et al. 2009; Sohn et al. 2007). Notably, although most of these studies have shown intracellular recognition of effectors, the contribution of HaRxL to virulence and their role in suppressing PTI responses can be studied using a bacterial effector delivery system (EDV) (Bailey et al. 2011; Cabral et al. 2011; Fabro et al. 2011; Sohn et al. 2007). In this system, the effector of interest is fused to the type III secretion signal of the *Pseudomonas syringae* effector AvrRps4 for its delivery directly into the plant cell. The AvrRps4 portion is cleaved from the chimera in planta between the second and third G in its GGGKRVY sequence, releasing the effector to play its role (Sohn et al. 2007).

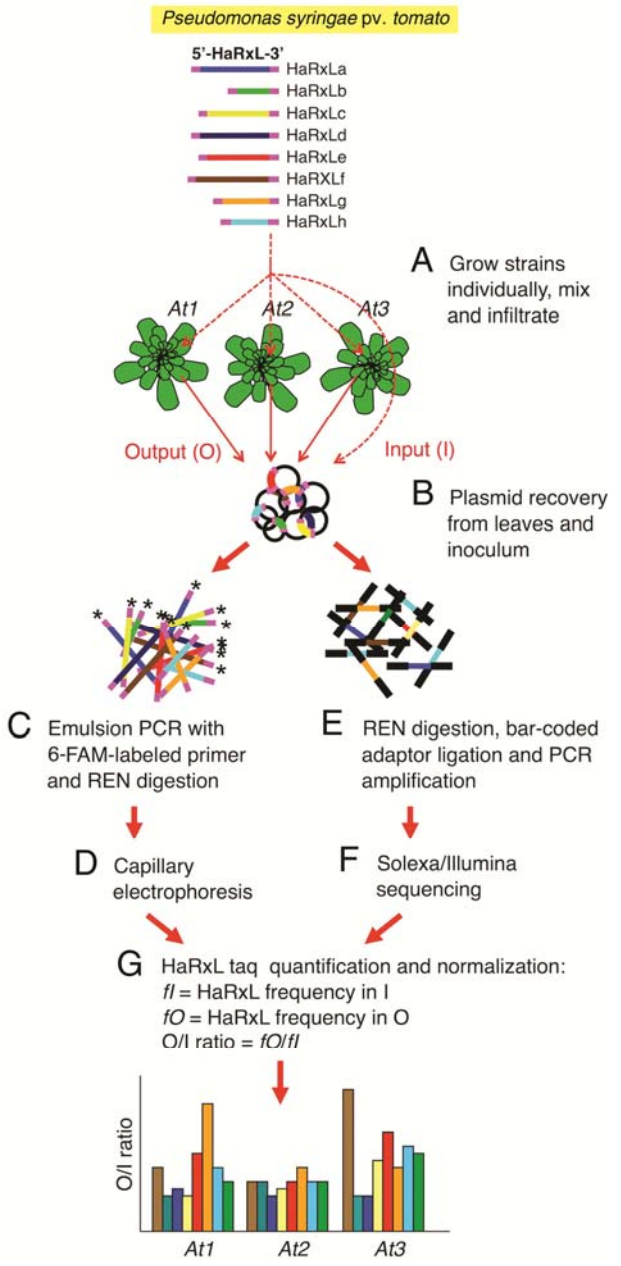

Fig. 1. Diagrammatic representation of in planta effector competition assays (IPECA). **A,** Bacterial strains are grown individually, mixed, and syringe infiltrated at 10^4 CFU/ml into leaves of 4- to 5-week-old *Arabidopsis* plants. **B,** Effector delivery system plasmids are recovered from input (approximately 5,000 CFU) and output samples (2,000 to 5,000 CFU/plate in IPECA–restriction endonuclease digestion coupled with capillary electrophoresis [RENCAP]; infected leaves in IPECA—restriction endonuclease digestion coupled with Solexa/Illumina multiplexed sequencing [RENSOL]). **C,** In IPECA-RENCAP, the high-confidence effectors (HaRxL) are amplified from samples by emulsion PCR using a 5′ 6-carboxyfluorescein (FAM)-labeled primer, and the amplicons digested with an enzymatic cocktail containing *Alw*NI, *Xma*I, and *Pml*I. **D,** Digested amplicons are quantified using capillary electrophoresis. **E,** In IPECA-RENSOL, the HaRxL are PCR amplified using a 3′ biotynilated primer, are bound to streptadivin beads, are cut with *Aci*I; an adaptor containing an *Mme*I site was ligated to the 5′ ends and digested with *Mme*I; and a barcoded adaptor was ligated to the 3′ ends. **F,** Sandwiched HaRxL tags are sequenced using Solexa/Illumina. **G,** Relative abundance of each effector in the IPECA is estimated by calculating the output/input (O/I) ratio.

In this study, we set out to rapidly identify HaRxL that contribute positively to pathogen fitness. We first developed methods to rapidly detect their abundance in complex mixed bacterial infections (Beuzon and Holden 2001; Macho et al. 2007) using effector delivery from *P. syringae* pv. *tomato* (Sohn et al. 2007) and medium- to high-throughput methods of effector detection. We designed two methods referred to here as in planta effector competition assays (IPECA) that allowed us to identify Emoy2 HaRxL that enhance bacterial multiplication in planta or show differential interactions with *Arabidopsis* accessions. We validate the predictions of IPECA for several of these effectors and provide evidence that they contribute to PTI suppression and localize to different plant subcellular compartments.

RESULTS

Development of a mixed infection assay.

We established an IPECA by inoculating complex mixtures of *P. syringae* pv. *tomato lux* strains each expressing an individual HaRxL in the EDV system (Baxter et al. 2010; Fabro et al. 2011; Sohn et al. 2007). For detection and quantification of individual HaRxL in complex mixtures, we designed medium- to high-throughput methods by using restriction endonuclease digestion coupled with capillary electrophoresis (RENCAP) or restriction endonuclease digestion coupled with Solexa/Illumina multiplexed sequencing (RENSOL) (Fig. 1).

IPECA-RENCAP: capillary electrophoresis of effectors in mixed infections detects contribution to virulence and differential interaction with *Arabidopsis* accessions.

We first determined the resistance or susceptibility of the founders of the multiparent advanced generation inter-cross (MAGIC) lines (Kover et al. 2009) to Emoy2 infection at 7 days postinoculation (dpi) (Holub 2006). These MAGIC lines allow rapid mapping of quantitative trait loci (QTL) associated with traits of interest (i.e., enhanced susceptibility). A set of 527 recombinant inbred lines that descended from the 19 founders is already available. These MAGIC lines and the 19 founders were already genotyped with 1,260 single-nucleotide polymorphisms and phenotyped for development-related traits (Kover et al. 2009). We then selected Col-0, Ws-0, Mt-0, Sf-2, Ler-0, Edi-0, and Bur-0 that show different resistance phenotypes, as well as the susceptible accession Tsu-0 to conduct IPECA-RENCAP (Supplementary Table S1). We syringe infiltrated these accessions with a mixture at equal numbers of *P. syringae* pv. *tomato lux* strains, each expressing a different effector: 19 HaRxL that show different DNA fragment sizes after digestion with a restriction enzyme mix. As controls, we included AvrRps4-AAAA, in which the KRVY motif is replaced by AAAA and that causes no change in bacterial multiplication in planta (Sohn et al. 2009); and HaRxL89-nls that carries the deletion of a direct repeat that allows its expression in *P. syringae* pv. *tomato lux* and does not cause any change in bacterial multiplication in planta (Figs. 2 and 3D; Supplementary Tables S2 and S3). We could not investigate the effect of full-length HaRxL89 in *P. syringae* pv. *tomato lux* because we were

unable to mobilize it despite repeated triparental matings and electrotransformation attempts. We also included the type-III-deficient mutant *P. syringae* pv. *tomato hrcC* expressing HaRxL143 to control for *P. syringae* pv. *tomato* growth in the absence of any type III effector. Expression of HaRxL143 allows detection and quantification of the *hrcC* mutant in the bacterial mixtures.

To compare effector abundance in planta, we isolated plasmid DNA from bacterial colonies recovered from leaf samples collected at 3 dpi, generated 6′-carboxyfluorescein (6-FAM)-labeled HaRxL fragments, and capillary electrophoresis was used to estimate their relative abundance and to calculate their output/input (O/I) ratios. We tested whether the observed ratios were significantly different from 1.00 using a Student's *t* test and adjusted the *P* values for multiple testing using the Benjamini and Hochberg test (1995). In addition, to determine whether a particular HaRxL was reproducibly enriched in the output sample, we introduced the two additional variables $f > 1$ and $f < 1$ that indicated the number of plants out of the total inoculated that showed O/I ratios higher than 1.00 and the number of plants out of the total inoculated that showed O/I ratios lower than 1.00, respectively. Finally, we classified the O/I ratio, $f > 1$, and $f < 1$ values into arbitrary ranks in a heat map to determine the strength of growth reduction or increase caused by each HaRxL (Fig. 2).

As expected, AvrRps4-AAAA (Sohn et al. 2009) and HaRxL143 expressed in *P. syringae* pv. *tomato hrcC* were not significantly enriched or depleted in the output sample from any *Arabidopsis* accession (Fig. 2). Statistical analysis showed that HaRxLL148 in Ws-0, HaRxL62 in Ler-0 and Bur-0, HaRxL14 in Sf-2, HaRxL68 in Bur-0, HaRxL73 in Bur-0, and HaRxL79 in Edi-0 had O/I ratios significantly higher than 1.00. HaRxL62 had mean ratios higher than 1.00 in the output sample of all other *Arabidopsis* accessions (Fig. 2), suggesting that, consistent with Fabro and associates (2011), it enhances bacterial multiplication in all accessions tested. However, the O/I ratios were significantly higher than 1.00 only for Ler-0 and Bur-0. Five other HaRxL were among the most enriched in the output samples of some accessions, as indicated by their mean O/I ratios: HaRxL4 and HaRxL73 in Edi-0, HaRxL75 in Tsu-0, HaRxLL464 in Col-0 and Sf-2, and HaRxL68 in Col-0 (Fig. 2). However, their O/I ratios were not statistically different from 1.00 and the results for HaRxLL464 and HaRxL68 in Col-0 were somewhat variable, as indicated by their $f > 1$ and $f < 1$ values (Fig. 2). HaRxL106 showed mean O/I ratios lower than 1.00 in all *Arabidopsis* accessions but statistical significance was not observed for Ler-0, Tsu-0, Mt-0, and Bur-0. The mean O/I ratio for HaRxL106 was also significantly lower than 1.00 in the output sample of Ws-0 using IPECA-RENSOL (Fig. 4A; Supplementary Table S4). HaRxL89-nls was not statistically different from 1.00 in any output sample, except for a depletion observed in Edi-0 (Fig. 3).

Because the mean O/I ratio and the $f > 1$ and $f < 1$ suggested that HaRxL75 was enriched in the output sample of Tsu-0, we decided to validate this IPECA-RENCAP prediction using standard growth assays, the rationale being that *P* value adjust-

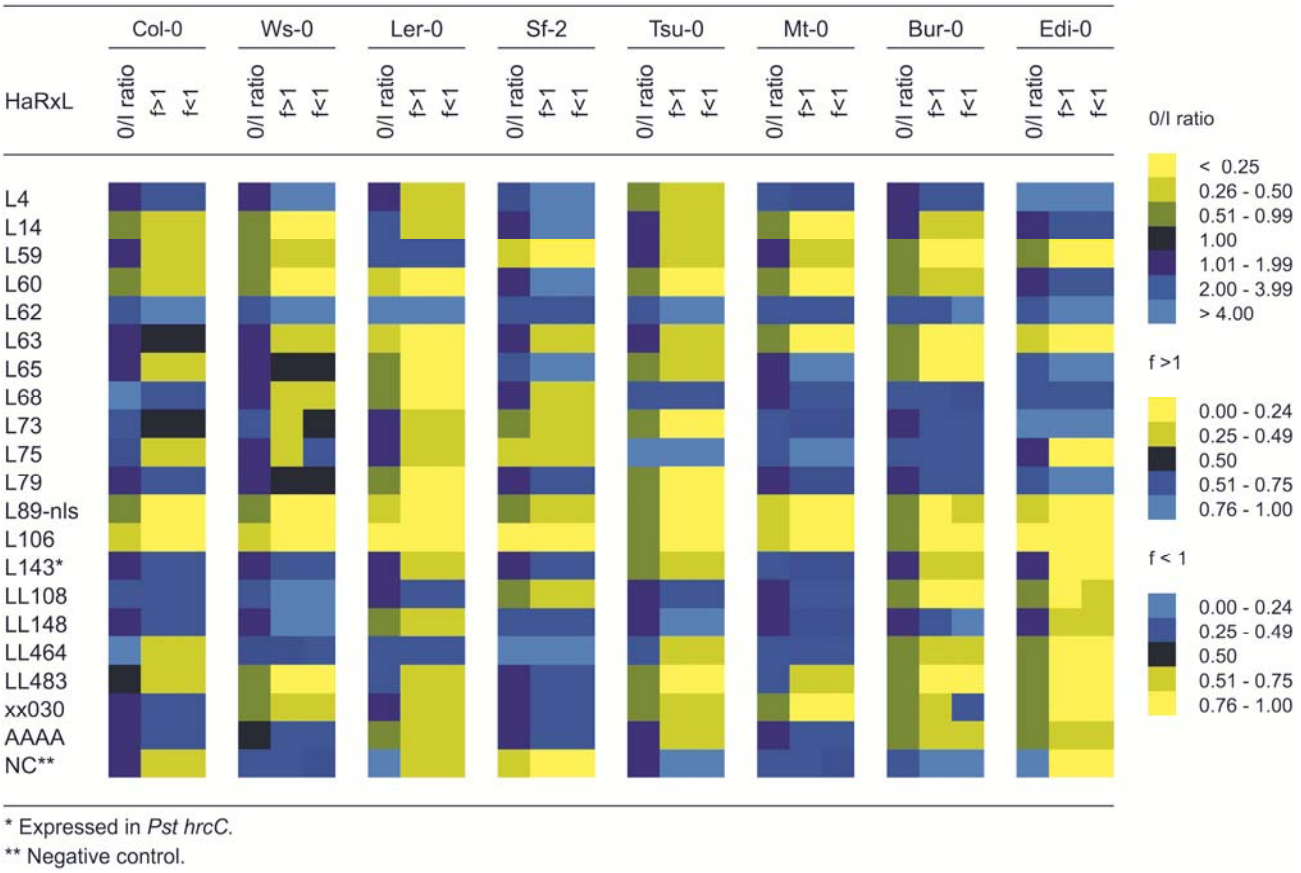

Fig. 2. Output/input (O/I) ratios for high-confidence effectors (HaRxL) in eight *Arabidopsis* accessions after in planta effector competition assay (IPECA)-restriction endonuclease digestion coupled with capillary electrophoresis (RENCAP). Heat map depicting the mean O/I ratios, $f > 1$, and $f < 1$ values for 20 HaRxL and AvrRps4-AAAA (AAAA) recovered from eight *Arabidopsis* accessions at 3 days after inoculation with the bacterial mixture. The $f > 1$ and $f < 1$ values indicate the number of plants out of the total inoculated that showed O/I ratios > 1.00 and the number of plants out of the total inoculated that showed O/I ratios < 1.00, respectively. Color codes represent O/I ratios, $f > 1$, and $f < 1$ values calculated for three independent experiments with three biological repetitions. Effector names are indicated using a simplified nomenclature without the initial HaRx.

ment for multiple testing often results in false negatives. As predicted by IPECA-RENCAP, HaRxL75 caused enhanced bacterial multiplication in Tsu-0 in standard growth assays (Fig. 3A). Expression of HaRxL75 in *P. syringae* pv. *tomato lux* also caused an enhancement of disease symptoms in Tsu-0 as compared with those caused by the strains carrying AvrRps4-AAAA (Fig. 3B). HaRxL75 also caused reductions in Col-0 when tested in standard growth assays (Fig. 3A). We also observed that, in Col-0, HaRxLL464 had O/I ratios significantly higher than 1.00 using IPECA-RENSOL (Fig. 4A) and caused enhanced growth in Col-0 (Fig. 4C) and Sf-2 but not in Tsu-0 or Edi-0 (Fig. 3C). Consistent with IPECA-RENCAP prediction, HaRxL89-nls did not cause significant changes in *P. syringae* pv. *tomato lux* growth in any of the four accessions (Fig. 3D). To further scrutinize the predictions obtained with IPECA-RENCAP, we compared mean O/I ratios with mean ratios (luciferase activity of the effector)/(luciferase activity of control strain) calculated from data reported by Fabro and associates (2011) (Supplementary Fig. S1). Although a high positive correlation between the two methods is not necessarily expected because detection of the contribution to virulence of some effectors has been shown to depend on the inoculation method (Badel et al. 2002; Brooks et al. 2004; Mittal and Davis 1995; Munkvold et al. 2009), we found that most Emoy2 effectors that show high O/I ratios in IPECA-RENCAP also show enhanced luciferase activity. The results of these comparisons with single-strain inoculation assays indicate that IPECA-RENCAP provides a good indication of the relative contribution of individual effectors to bacterial multiplication in planta.

IPECA-RENSOL: multiplex tag sequencing of mixed infections identifies effectors that contribute to pathogen multiplication.

Because the number of strains that can be assayed in IPECA-RENCAP is constrained by the detection based on HaRxL sizes, we sought to detect and quantify the HaRxL inserts based on their unique sequences using Illumina tag sequencing. We

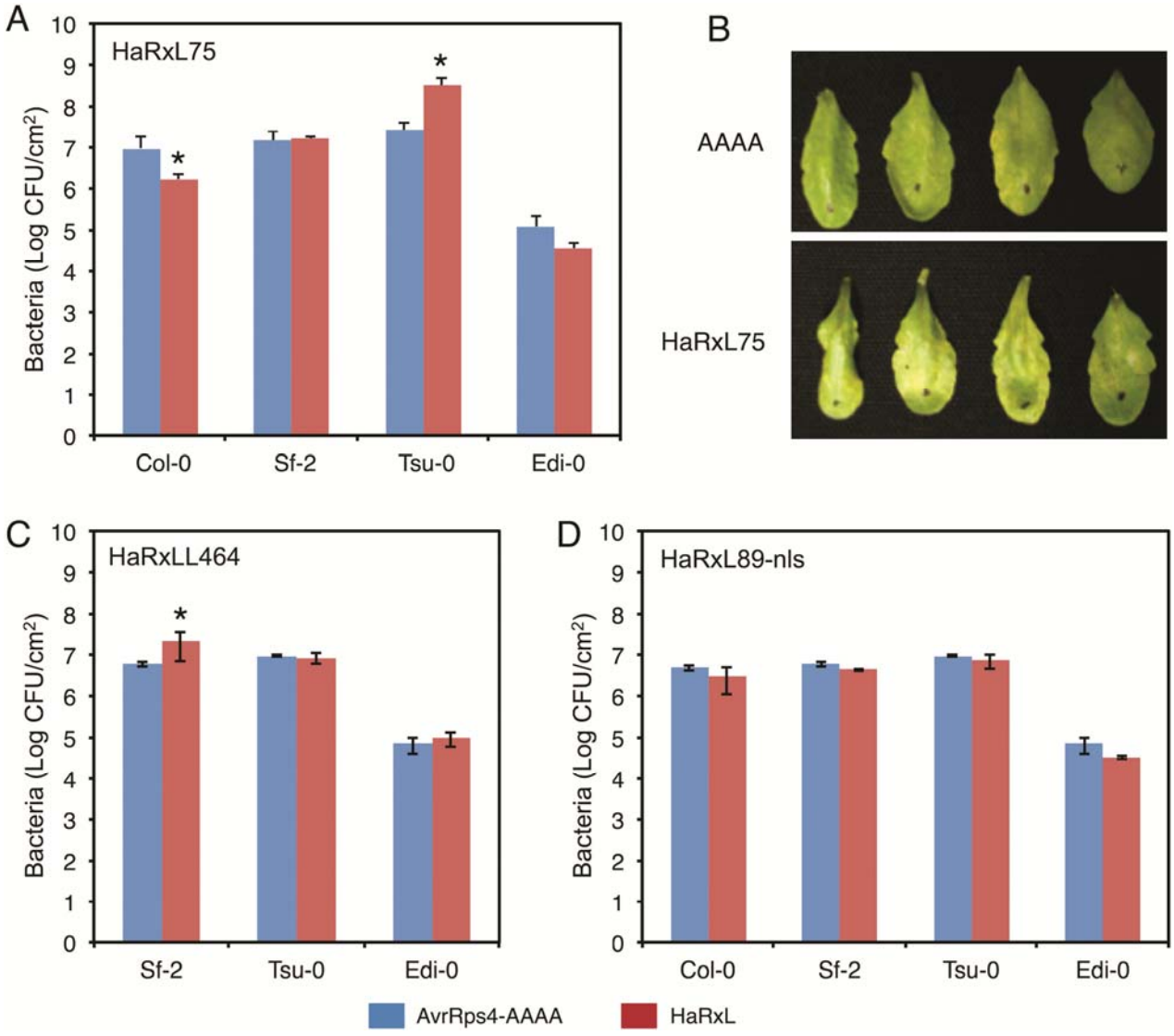

Fig. 3. Enhanced bacterial multiplication caused by HaRxL75 in Tsu-0 and HaRxLL464 in Sf-2. Multiplication of *Pseudomonas syringae* pv. *tomato lux* strains expressing **A,** HaRxL75; **C,** HaRxLL464; and **D,** HaRxL89-nls in Col-0, Sf-2, Tsu-0, or Edi-0. **B,** Disease symptoms caused by *P. syringae* pv. *tomato lux* strains expressing HaRxL75 or AvrRps4-AAAA (AAAA, negative control) in Tsu-0. *Arabidopsis* plants (4 to 5 weeks old) were syringe infiltrated with *P. syringae* pv. *tomato lux* at 10^5 CFU/ml delivering AvrRps4-AAAA (blue bars) or the high-confidence effectors (HaRxL) (red bars). Bacterial growth was measured in leaves at 3 days postinoculation by colony counting on selective medium. Vertical bars represent standard errors of mean bacterial counts from three replicates. Asterisks indicate statistically significant differences between HaRxL and control strains (Student's *t* test *P* values ≤ 0.04). Similar results were obtained in three independent experiments with three biological repetitions.

syringe infiltrated *Arabidopsis* Col-0 and Ws-0 leaves with a mixture of equal numbers of 27 randomly chosen *P. syringae* pv. *tomato lux* carrying different HaRxL in the EDV system, a subset of strains with little overlap with that used in IPECA-RENCAP. We also included *P. syringae* pv. *tomato lux* strains expressing β-glucuronidase (GUS) or yellow fluorescent protein (YFP) or carrying an empty pEDV to control for normal *P. syringae* pv. *tomato lux* growth, and *P. syringae* pv. *tomato hrcC* expressing HaRxL67. Expression of HaRxL67 in the *hrcC* mutant allows its detection and quantification in the bacterial mixture using the effector sequence as a tag. Plasmid DNA was isolated from input and output samples, and 3′ barcoded HaRxL tags were generated and sequenced using Solexa/Illumina technology.

There was considerable variation between the tag counts from output Col-0, Ws-0, and the input *P. syringae* pv. *tomato lux* samples. The *P. syringae* pv. *tomato* input sample accounted for 79.526% of the 3,851,930 tags, whereas tags from Col-0 and Ws-0 samples accounted for 0.005 and 0.200% tags, respectively (Fig. 4A). As expected, *HaRxL67*, which was expressed in the *P. syringae* pv. *tomato hrcC* mutant, was among the lowest-abundance sequence tags in both Col-0 and Ws-0. In fact, we could not detect any *HaRxL67* tags in the output samples from Col-0. The O/I ratio for controls expressing EVD5, GUS, and YFP were not significantly different from 1.00, except for an O/I ratio of 6.82 for YFP significantly different from 1.00 in Col-0. Therefore, we arbitrarily established a cut-off O/I ratio of 10.00 to predict a major positive effect on *P. syringae* pv. *tomato lux* growth. The O/I ratios for HaRxLL441 in both Ws-0 (51.96; P = 0.00008) and Col-0 (23.35; P = 0.00451) and for HaRxLL464 in Col-0 (63.94; P = 0.00618) were significantly higher than 1.00 (Fig. 4A). These results suggested that HaRxLL441 enhances bacterial multiplication in both Ws-0 and Col-0 and HaRxLL464 does so in Col-0. We also noticed that the O/I ratio for HaRxL22 was high in Ws-0 (29.65) but its statistical significance was lost after correction for multiple testing (unadjusted

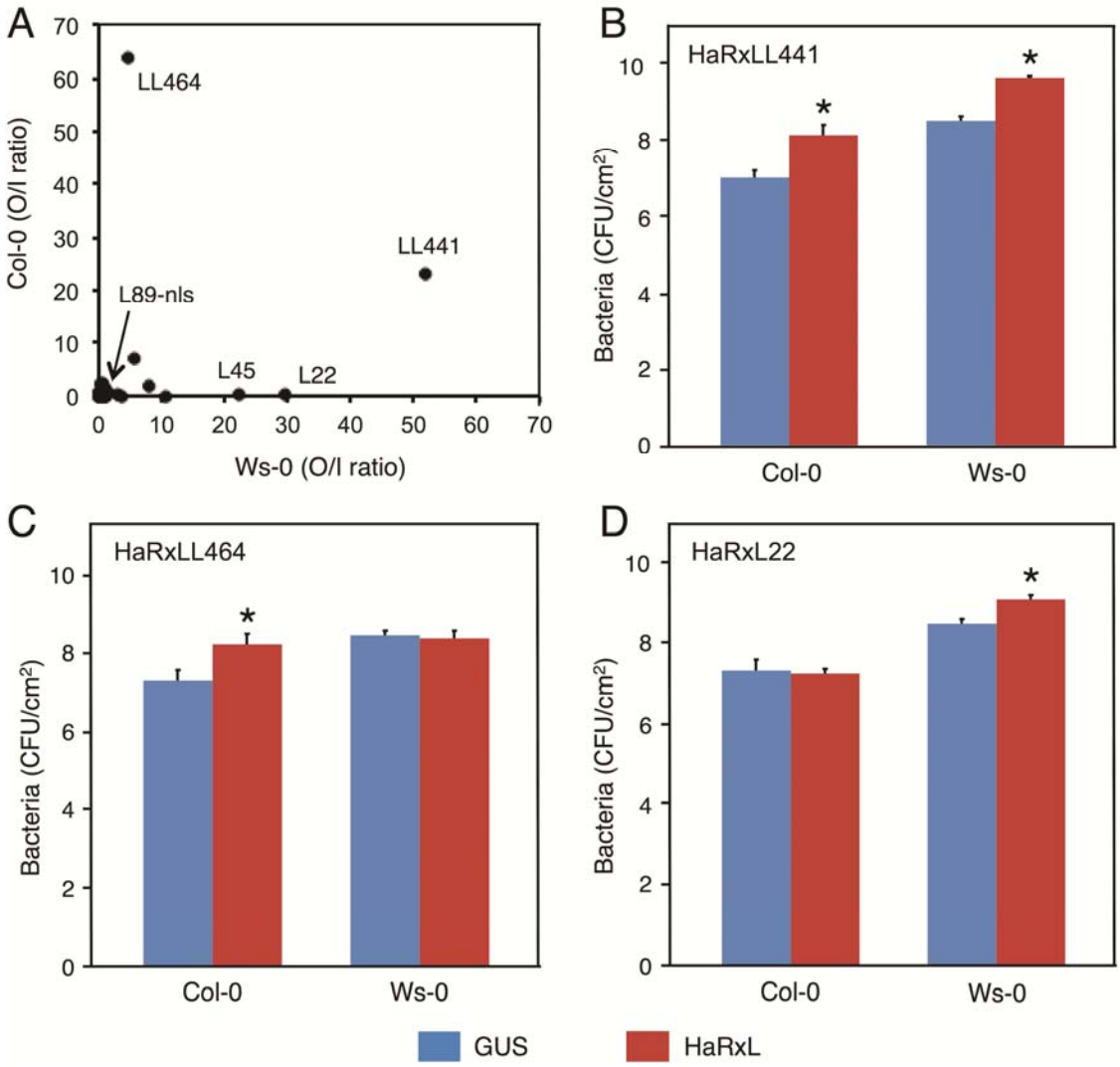

Fig. 4. In planta effector competition assay (IPECA)-restriction endonuclease digestion coupled with Solexa/Illumina multiplexed sequencing (RENSOL) detects high-confidence effector (HaRxL) contributions to bacterial multiplication and their differential interaction with Ws-0 and Col-0. **A**, Correlation between the output/input (O/I) ratios for 28 HaRxL, yellow fluorescent protein, and β-glucuronidase (GUS) controls recovered from Ws-0 and Col-0 leaves at 3 days after inoculation with the bacterial mixture at 10^4 CFU/ml. Labels indicate HaRxL that are enriched in the output sample of at least one *Arabidopsis* accession using a simplified nomenclature without the initial HaRx. Arrow indicates that the mean O/I ratio for HaRxL89-nls was close to 1.00 in both accessions. **B** to **D**, Multiplication in Col-0 and Ws-0 of *Pseudomonas syringae* pv. *tomato lux* expressing **B**, HaRxLL441; **C**, HaRxLL464; and **D**, HaRxL22. For B–D, 4- to 5-week-old *Arabidopsis* plants were syringe infiltrated with *P. syringae* pv. *tomato lux* at 10^5 CFU/ml delivering GUS (negative control, blue bars) or the HaRxL (red bars). Bacterial growth was measured in leaves at 3 days postinoculation by colony counting on selective medium. Vertical bars represent standard errors of mean bacterial counts from three replicates. Asterisks indicate statistically significant differences between HaRxL and control strains (Student's t test P values ≤ 0.01). Similar results were obtained in three independent experiments with three biological repetitions.

P = 0.0150; adjusted P = 0.0581). Inoculation of *Arabidopsis* plants with HaRxLL441 and HaRxLL464 in standard growth assays mirrored the results from the mixed infection. Compared with a control expressing GUS, HaRxLL441 enhanced growth by 10-fold in both Col-0 and Ws-0 (Fig. 4B), and HaRxLL464 caused a 10-fold increase in *P. syringae* pv. *tomato lux* growth in Col-0 but not in Ws-0 (Fig. 4C). We also inoculated HaRxL22 in both Col-0 and Ws-0 plants in order to rule out the possibility that the Benjamini and Hochberg adjustment had resulted in a false negative, a common effect of corrections for multiple testing. HaRxL22 caused a fivefold growth increase only in Ws-0 (Fig. 4D). Taken together, the results show that IPECARENSOL of mixed infections using the EDV system can predict effectors that enhance bacterial multiplication in planta.

The enhanced growth in planta caused by HaRxLL464, HaRxLL441, HaRxL22, and HaRxL75 is not the result of an intrinsic enhanced bacterial growth.

We observed a reproducible retardation in the growth of bacterial cells expressing HaRxL compared with those expressing AvrRps4-AAAA when strains were grown in axenic liquid culture (Supplementary Fig. S2). Similar results were obtained when the bacterial strains were grown on solid medium and their growth assayed using luciferase activity. These results indicate that the enhanced growth caused by HaRxL22, HaRxLL441, HaRxL75, and HaRxLL464 is specific to their role during the interaction with the plant but also that any decrease of growth in planta caused by the effector must be interpreted cautiously and may not be associated with a strong recognition by the plant immune system. Indeed, we were unable to detect any significant difference between the tissue collapse elicited by *P. syringae* pv. *tomato lux* strains expressing HaRxL75 and AvrRps4-AAAA at 24 to 72 h after infiltration into Col-0 leaves. The frequency of tissue collapse caused by *P. syringae* pv. *tomato lux* expressing HaRxL75 was similar in both Tsu-0 and Col-0, suggesting no differential recognition in the two accessions. Similar results were obtained when the effectors were expressed in *P. fluorescens* EtHan (Thomas et al. 2009) (data not shown).

Some selected effectors show amino acid sequence similarities to other predicted effectors or contain motifs conserved in proteins of predicted function.

We then investigated possible biochemical functions of the select group of HaRxL based on amino acid sequence comparisons. We found that the HaRxL89-predicted protein shares 52% amino acid identity with HpAvh341. The highest similarity between the two predicted proteins extends from the start site until a putative RxLR motif (RQLR), after which the two proteins diverge considerably. Interestingly, the region of homology in HpAvh341 has been shown to be functional in translocating *Phytophthora sojae* Avr1b (Dou et al. 2008b). HaRxL75-predicted protein shows 35% amino acid identity with a predicted RxLR effector from *P. infestans* T30-4 (XP_002898703.1), and 43, 41, and 41% amino acid identity to the *P. sojae* *Ps*Avh7a, *Ps*Avh7b1, and *Ps*Avh7c, respectively. Most of these similarities also reside toward the N-terminal portion of the proteins (Supplementary Fig. S3). The C-terminus of HaRxLL441 shows sequence similarity to microbial proteins involved or predicted to be involved in redox reactions, such as dehydrogenases, dehydratases, and epimerases, and to members of the NmrA family (Supplementary Fig. S4). Furthermore, HaRxLL441 is predicted to contain a NADB Rossmann superfamily fold present in NAD(P)H/NAD(P)$^+$ binding proteins, including dehydrogenases or reductases. Nonetheless, HaRxLL441 is most similar to a conserved hypothetical protein from *P. infestans* T30-4 (66% identity). HaRxL22 shows significant sequence identity to many predicted RxLR effectors from *P. infestans* and *P. sojae* (Supplementary Fig. S5). Multiple sequence alignment using AlignX and motif searches using MEME revealed the presence of three conserved motifs in members of the HaRxL22 protein family; each motif can be present in up to five copies in a family member. We did not find any significant sequence similarity of HaRxLL464 or HaRxL89 to any protein from other organisms in the databases, suggesting that these HaRxL are specific to *Hyaloperonospora* spp.

Five selected HaRxL suppress callose deposition caused by *Pseudomonas syringae* pv. *tomato* ΔCEL in Col-0 and restore ETI suppressed by *P. fluorescens* in *Nicotiana benthamiana*.

The enhanced bacterial multiplication in planta caused by HaRxLL464, HaRxL75, HaRxLL441, and HaRxL22 prompted us to investigate whether they could suppress PTI using assays previously shown for bacterial, fungal, and oomycete effectors (DebRoy et al. 2004; Hauck et al. 2003; Kelley et al. 2010; Underwood et al. 2007; Zhang et al. 2007). We also included HaRxL89-nls expressed in *P. syringae* pv. *tomato* ΔCEL and full-length HaRxL89 in *P. fluorescens* EtHan. We first confirmed expression of these five HaRxL during Emoy2 infection by reverse-transcriptase polymerase chain reaction (PCR) (Supplementary Fig. S6). Sequence tags for these effectors were found in a large screening for HaRxL expressed during the interaction of Emoy2 with *Arabidopsis* (Fabro et al. 2011). We tested the five effectors and the control strains expressing ATR13 or HopM1 and its customary chaperone, SchM1 (Badel et al. 2003, 2006), for their ability to suppress callose deposition elicited by *P. syringae* pv. *tomato* ΔCEL PAMPs (DebRoy et al. 2004; Sohn et al. 2007). Consistent with previous reports, compared with *P. syringae* pv. *tomato* ΔCEL, expression of HopM1-SchM1 and ATR13 caused 85 and 68% reduction, respectively, in callose deposition (Fig. 5A) (DebRoy et al. 2004; Sohn et al. 2007). Expression of all five HaRxL in *P. syringae* pv. *tomato* ΔCEL caused reduction in the number of callose deposits ranging from 27% (HaRxL22) to 46% (HaRxL75) (Fig. 5A).

The tissue collapse associated with the ETI response elicited by pathogenic bacteria in a nonhost is suppressed if the same area is previously infiltrated with nonpathogenic bacteria. Elicitation of PTI by the nonpathogenic bacterium restricts the translocation of TTSS effectors by the pathogenic bacterium and this restriction results in suppression of tissue collapse (Crabill et al. 2010; Nguyen et al. 2010; Oh et al. 2010). If the nonpathogenic bacterium expresses an effector and the tissue collapse associated with the ETI response is observed, the effector is a suppressor of PTI. In contrast, if the tissue collapse is not observed, the effector does not suppress PTI (Crabill et al. 2010; Nguyen et al. 2010; Oh et al. 2010). We infiltrated *P. fluorescens* EtHan into *Nicotiana benthamiana*, allowed for development of the PTI response during 7 h, and then infiltrated *P. syringae* pv. *tomato* DC3000 in an overlapping area and looked for the development of tissue collapse at 72 h. *P. fluorescens* EtHan abolished elicitation of HR in the area overlapping the secondary *P. syringae* pv. *tomato* DC3000 infiltration, indicating that *P. fluorescens* EtHan elicited the PTI response in *N. benthamiana* (Fig. 5B). Expression of AvrRps4-AAAA in *P. fluorescens* EtHan did not restore elicitation of HR by *P. syringae* pv. *tomato* DC3000 in the overlapping area, indicating that it does not suppress the PTI response elicited by *P. fluorescens* EtHan in *N. benthamiana*; therefore, we used this nonfunctional bacterial effector allele as a negative control (Fig. 5B). Expression in *P. fluorescens* EtHan of $AvrPtoB_{308\text{-}553}$ (Abramovitch et al. 2003), a derivative of

AvrPtoB expressing amino acids 308 to 553 of AvrPtoB, did not elicit an HR in *N. benthamiana* at a high inoculum dose and restored the tissue collapse elicited by *P. syringae* pv. *tomato* DC3000 in the overlapping area, indicating that it suppresses the PTI response elicited by *P. fluorescens* EtHan in *N. benthamiana* (Fig. 5B). Therefore, we used $AvrPtoB_{308-553}$ as a positive control in experiments aimed at investigating whether HaRxLL464, HaRxL75, HaRxLL441, HaRXL22, and HaRxL89 can suppress the PTI response elicited by *P. fluorescens* EtHan in *N. benthamiana.* Expression of all five HaRxL in *P. fluorescens* EtHan restored the HR elicited by *P. syringae* pv. *tomato* DC3000 in the overlapping area, indicating that they can restore the ability of *P. syringae* pv. *tomato* DC3000 to translocate bacterial effectors into *N. benthamiana* cells and, hence, suppress the PTI response elicited by *P. fluorescens* EtHan in *N. benthamiana*. The magnitude of restoration of the HR in the overlapping area caused by the HaRxL varied within and between experiments (Fig. 5B).

Five Emoy2 HaRxL localize to different subcellular compartments in *N. benthamiana.*

We then investigated where in the plant cell these HaRxL are targeted. We delivered all five effectors as N- and C-termini in-frame fusions with green or red fluorescent protein (GFP or RFP, respectively) into *N. benthamiana* using *Agrobacterium*-mediated transient expression. We also delivered GFP as control. As expected, GFP showed nuclear-cytoplasmic localization with exclusion from the nucleolus. Our results indicate that these five effectors localize to different subcellular compartments. HaRxL75 localizes exclusively to the plasma membrane (Supplementary Fig. S7); HaRxL89 localizes to the nucleus and, preferentially, in the nucleolus; and HaRxLL441 and HaRxL22 show nuclear-cytoplasmic distribution with nucleolar exclusion (Fig. 6). We made four different fusions for each HaRxL: C-terminal fusion with GFP, N-terminal fusion with GFP, C-terminal fusion with RFP, and N-terminal fusion with RFP. We transiently expressed at least three different constructs of each fusion in *N. benthamiana* and did not observe any difference in the subcellular localization pattern for any HaRxL. We checked the stability of transiently expressed GFP-tagged effector chimeras using Western blots in order to exclude any misinterpretation of the effector localization. All full-length GFP-tagged effectors were detected (Supplementary Fig. S8). However, for some effectors, we observed site-specific cleavage of the GFP:HaRxL chimeric protein. This is the case for GFP:HaRxLL464, whose nuclear-cytoplasmic localization could be explained by free diffusion of released GFP after cleavage of the chimera. Therefore, we could not obtain conclusive evidence for the subcellular localization of HaRxLL464. GFP:HaRxL89 also showed cleavage, which could explain the nucleoplasmic localization of the GFP signal. GFP:HaRxL75 showed some partial degradation, which may be due to the protein extraction method, given its plasma membrane localization. GFP:HaRxL22 and GFP:HaRxLL441 did not show cleavage or degradation but they are expressed at very low levels. The localization of a different subset of Emoy2 HaRxL to these and other subcellular compartments was reported recently (Caillaud et al. 2012). These results suggest that oomycete effectors are able to suppress the PTI response by different molecular mechanisms in different subcellular compartments.

DISCUSSION

In order to identify *H. arabidopsidis* effectors that contribute to pathogen fitness, we developed IPECA for medium- to high-throughput screening using heterologous expression in

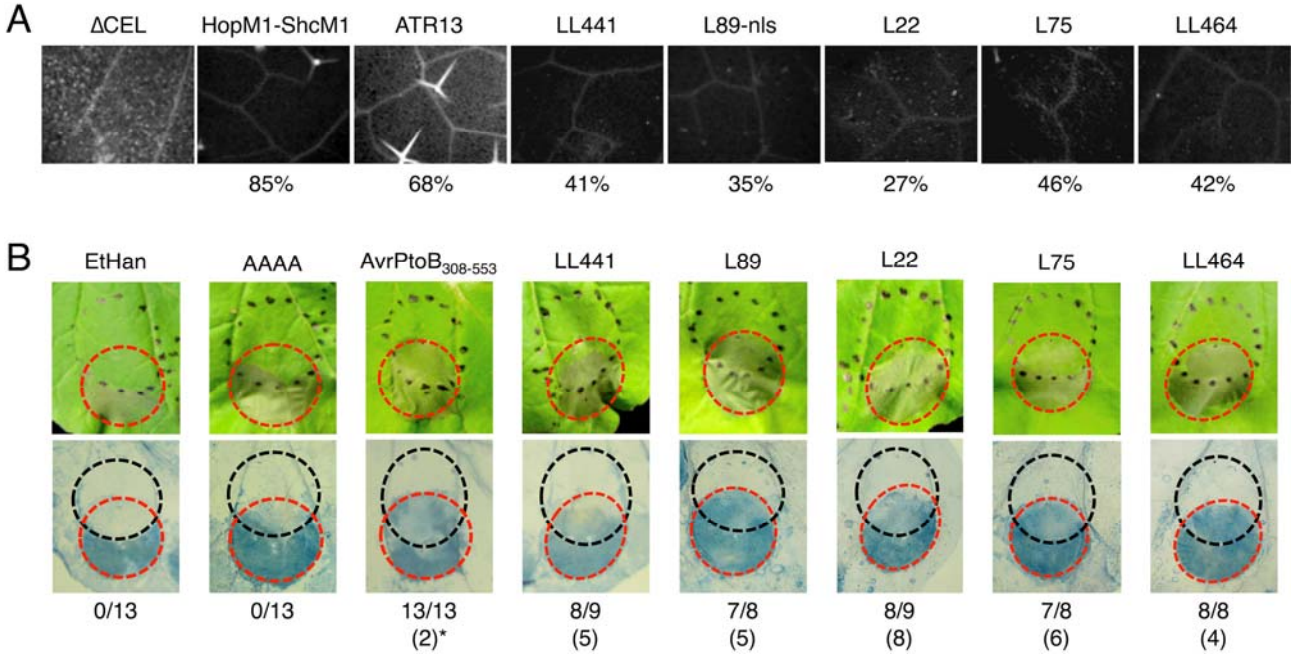

Fig. 5. Five selected high-confidence effectors (HaRxL) suppress pathogen-associated molecular pattern-triggered immunity in *Arabidopsis* and *Nicotiana benthamiana.* **A,** Callose deposits elicited in Col-0 leaves at 12 h after infiltration with suspensions at an optical density at 600 nm (OD_{600}) = 0.05 of *Pseudomonas syringae* pv. *tomato* ΔCEL expressing HopM1-ShM1, ATR13 (positive controls), or HaRxL. Bacteria were infiltrated into the abaxial side of leaves of 5-week-old plants and callose deposits were counted on 20 leaf discs collected from different plants. Values indicate the percentage of callose deposition as compared with *P. syringae* pv. *tomato* ΔCEL. **B,** Restoration of effector-triggered immunity suppressed by *P. fluorescens* in *N. benthamiana*. Suspensions at OD_{600} = 0.2 of *P. fluorescens* EtHan strains expressing AvrRps4-AAAA (AAAA, negative control), $AvrPtoB_{308-553}$ (positive control), or the HaRxL were infiltrated into the abaxial side of *N. benthamiana* leaves (black dotted circle) and, 7 h later, a suspension at OD_{600} = 0.02 of *P. syringae* pv. *tomato* DC3000 was infiltrated in an overlapping area (red dotted circle). Top panel, pictures taken at 3 days postinoculation. Lower panel, the same leaves stained with Trypan blue. Values indicate the number of times suppression of tissue collapse was observed out of the total number of leaves infiltrated in three independent experiments. The number of partial suppressions of tissue collapse is indicated in parenthesis. Effector names are indicated using a simplified nomenclature without the initial HaRx.

and delivery by *P. syringae* pv. *tomato lux*, bacterial mixed infections, and effector detection and quantification using either capillary electrophoresis or Illumina sequencing. These assays allowed us to identify four HaRxL that enhance bacterial multiplication in some *Arabidopsis* accessions but not in others. Our screening serendipitously also revealed an effector that shows signatures of being secreted, translocated, and localized to the plant nucleus.

We applied IPECA to founders of the MAGIC lines in order to open possibilities to rapidly map QTL for plant susceptibility genes. In order to undertake QTL mapping studies, the appropriate combination of *Arabidopsis* accessions should be chosen, taking into account their resistance to *P. syringae* pv. *tomato*. For example, if a susceptibility target for HaRxL75 were to be looked after, the combination Tsu-0xSf-2 sounds more appropriate than Tsu-0xEdi-0, given the level of resistance exhibited by Edi-0 toward *P. syringae* pv. *tomato* (Fig. 3). This resistance could hinder the possibility to detect enhanced or reduced bacterial multiplication caused by effectors. Therefore, IPECA predictions must be validated using standard methods to individual effectors. IPECA have the potential to be applied to any host microbe as well as to microbial diversity and evolution studies.

Although direct comparison between the study conducted by Fabro and associates (2011) and ours is difficult because of differences in the inoculation method (spray inoculation versus syringe infiltration) and in the nature of the assay (enhanced luciferase activity caused by a particular effector in single-strain inoculations versus competitiveness of the same effector in complex mixed infections), it is worth discussing common and contrasting findings. It is remarkable that most Emoy2 effectors that show high O/I ratios in IPECA-RENCAP also show enhanced luciferase activity in single-strain inoculation assays. This verifies a selected subset as strong candidates for further studies aimed at understanding oomycete effector function. We observed that HaRxL62 was a good competitor in competition assays conducted in all *Arabidopsis* accessions tested in IPECA-RENCAP. These results are consistent with the HaRxL62 enhancement of luciferase activity and bacterial multiplication in planta reported by Fabro and associates (2011) for all accessions included in their study. Consistent with its poor competition in Col-0, Fabro and associates (2011) reported that expression of HaRxL106 in *P. syringae* pv. *tomato lux* causes an overall decrease in both luciferase activity and bacterial growth in this accession. Notably, HaRxL106 suppresses immunity when expressed as a transgene in Col-0 (Fabro et al. 2011), indicating that different effector delivery systems can lead to different outcomes. Fabro and associates (2011) further reported an overall increase of luciferase activity caused by HaRxL106 in Ler-0, Tsu-0, and Ws-0 using luciferase activity as a measure of bacterial growth in planta, which contrasted with poor competition of HaRxL106 on these accessions in our assays, where bacteria were infiltrated into the apoplast. These observations suggest that HaRxL106 may play a role in promoting host colonization early during infection (Melotto et al. 2006). Further characterization of HaRxL62 and HaRxL106, as well as other effectors that enhance bacterial multiplication in some ecotypes, will be published elsewhere.

Consistent with our results, Fabro and associates (2011) detected enhanced luciferase activity caused by expression of HaRxLL464 in Col-0 but not significant enhancement in Ws-0 and by expression of HaRxL75 in Tsu-0 but not in Col-0. Moreover, the contribution of HaRxLL464 to virulence was verified by stably expressing this HaRxL in Col-0 plants (Fabro et al. 2011). These results suggest that HaRxLL464 and HaRxL75 play their roles during the *P. syringae* pv. *tomato lux* and *Arabidopsis* interaction at a stage later than epiphytic growth. How-

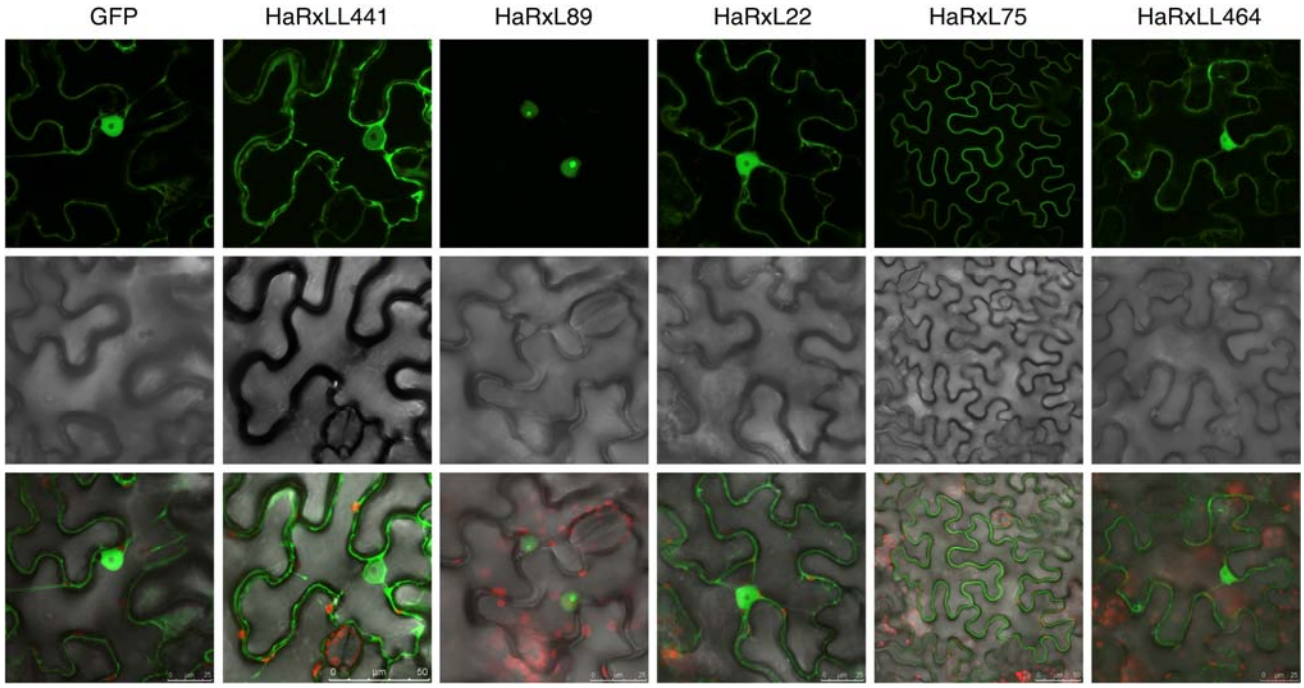

Fig. 6. Five selected high-confidence effectors (HaRxL) localize to different subcellular compartments in *Nicotiana benthamiana*. Suspensions at an optical density at 600 nm = 0.2 of *Agrobacterium tumefaciens* strains expressing N- or C-terminal fusions with green fluorescent protein (GFP) or red fluorescent protein (RFP) fused in frame to the HaRxL were syringe infiltrated into the abaxial side of 3- to 4-week-old *N. benthamiana* leaves and fluorescence was observed after 2 to 3 days with a Leica confocal microscope. Top panel, fluorescence image; middle panel, brightfield image; bottom panel, merged image. Localization patterns: GFP, nucleus and cytoplasm with nucleolar exclusion; HaRxL75, plasma membrane; HaRxL89, nucleus and nucleolus; HaRxLL464, HaRxL22, and HaRxLL441, nuclear-cytoplasmic with nucleolar exclusion. At least three independent constructs of both GFP and RFP fusions to the C and N terminus of each effector were tested, with similar results.

ever, Fabro and associates (2011) reported reduced luciferase activity caused by HaRxLL441 in Ws-0 but no effect in Col-0, suggesting that its contribution to virulence depends upon bacteria reaching the apoplast. Also contrasting with our observations, Fabro and associates (2011) reported enhanced luciferase activity in Col-0 and no effect in Ws-0 caused by HaRxL22. It is tempting to speculate that the magnitude of the contribution to virulence of a particular effector in a particular plant species or accession depends on its affinity for the plant target. The contribution to virulence by these HaRxL in some accessions but not in others suggests allelic variations in the plant susceptibility targets and that HaRxL are under selection pressure to co-evolve with them. Our results indicate that HaRxL75, HaRxL441, and HaRxL22 are conserved in *Phytophthora* spp., suggesting that they could play key roles for oomycete biotrophic lifestyle. In contrast, HaRxLL464 and HaRxL89 may contribute to adaptations specific to *Hyaloperonospora* spp. Further analysis of these HaRxL orthologs in *H. arabidopsidis* and other oomycete species will shed light into the mechanisms that shape HaRxL evolution.

We observed that expression of HaRxL75 in *P. syringae* pv. *tomato lux* caused reduction of bacterial multiplication in Col-0. However, we could not detect any increase in either the magnitude of cell death or the frequency of macroscopic or microscopic cell death caused by *P. syringae* pv. *tomato lux* or *P. fluorescens* EtHan expressing HaRxL75 as compared with control strains. These results could be explained in two ways: i) the recognition of HaRxL75 in Col-0 is not associated with the development of HR, supporting the notion that HR is not always required for resistance (Gassmann et al. 1999; Yu et al. 1998), or ii) the reduced growth of *P. syringae* pv. *tomato lux* carrying HaRxL75 is the result of its effect on delaying *P. syringae* pv. *tomato lux* multiplication. It is remarkable that HaRxL75 can cause a significant increase of *P. syringae* pv. *tomato lux* multiplication in Tsu-0, suggesting a functional susceptibility target to be present in this accession but not in Col-0. Similar observations for HaRxL22 and HaRxLL441 in Ws-0 and Col-0 suggest that the identification of plant proteins that interact with HaRxL in planta will shed light on the mechanisms by which they contribute to virulence only in some accessions. In addition, the analysis of the variability of these plant proteins among *Arabidopsis* accessions will provide insights into the mechanisms that shape the arms race between oomycete effectors and their susceptibility targets.

We found that HaRxL75, HaRxL89, HaRxLL441, HaRxLL464, and HaRxL22 suppress callose deposition elicited by *P. syringae* pv. *tomato* ΔCEL in *Arabidopsis* and restored ETI suppressed by *P. fluorescens* EtHan in *N. benthamiana*, pointing to their contribution to virulence by suppression of PTI, as already shown for bacterial effectors (Hann and Rathjen 2007; Zhang and Zhou 2010). The suppression of PTI in *N. benthamiana* and *Arabidopsis* by HaRxL suggests that their plant targets are conserved between these two species. Alternatively, they could suppress PTI via more than one mechanism. PTI suppression in Col-0 was not necessarily correlated with an enhanced bacterial multiplication caused by the HaRxL in the same accession. Notably, the ability of an effector to suppress plant defense responses is not always correlated with a detectable enhancement of bacterial multiplication in planta using standard growth curve assays. For example, HopM1 is able to suppress callose deposition in *Arabidopsis* leaves (DebRoy et al. 2004) and basal resistance in *N. benthamiana* (Oh and Collmer 2005) but its deletion in *P. syringae* pv. *tomato* DC3000 does not cause any reduction in bacterial growth in tomato (Badel et al. 2003). In addition, the majority of *P. syringae* pv. *tomato* DC3000 effectors are able to suppress plant defense responses (Guo et al. 2009) but a clear positive contribution of most of these effectors to bacterial multiplication in planta remains to be shown. It is also possible that the contribution of these HaRxL to virulence in some accessions is so subtle that it cannot be detected using the traditional bacterial counting methods (e.g., HopAA1-1) (Badel et al. 2002). Finally, it is also possible that they just do not contribute to bacterial multiplication in planta, yet they suppress defense responses in order to contribute to other components of parasitism (Badel et al. 2003).

The ability of oomycete effectors to suppress PTI elicited by bacterial PAMPs suggests the existence of common signaling pathways used by the plant surveillance system to mount the resistance response against pathogens of diverse taxonomic groups. In line with this notion, it was recently shown that the receptor-like kinase SERK3/BAK1 is required for basal resistance against *P. infestans* in *N. benthamiana* (Chaparro-Garcia et al. 2011), and the bacterial effector AvrPtoB targets the LysM receptor kinase CERK1 to promote virulence (Gimenez-Ibanez et al. 2009). CERK1 and two other lysin-motif proteins, LYM1 and LYM3, have recently been shown to mediate bacterial peptidoglycan sensing and immunity to bacterial infection (Willmann et al. 2011). Notably, HaRxL75, HaRxL89, HaRxLL441, and HaRxL22 localize to different subcellular compartments of the plant cell, suggesting that PTI suppression by oomycetes is multilayered, as reported for bacterial pathogens (Hann and Rathjen 2007; Zhang and Zhou 2010). For instance, the *P. syringae* pv. *tomato* effectors AvrPtoB and HopM1 suppress callose deposition by targeting different layers of PTI; namely, AvrPtoB targets receptor kinases such as BAK1 and CERK1 whereas HopM1 targets vesicle trafficking by regulating the levels of AtMin7 (Zhang and Zhou 2010).

Based on the plasma membrane localization of GFP-tagged HaRxL75, it is tempting to speculate that HaRxL75 suppresses PTI by interfering with activities of the plant immune response associated with the plasma membrane, perhaps by interfering with the function of receptor-like kinases, receptor-like proteins, or co-receptors. The subcellular localization of GFP-tagged HaRxL22 and HaRxLL441 begs the questions of how they might interfere with PAMP recognition. HaRxLL441 is predicted to contain an NADB-Rossmann superfamily fold involved in NAD(P)H/NAD(P)$^+$ binding (Rossmann et al. 1974) and shows amino acid sequence similarity to members of the NmrA family. NmrA is a negative transcriptional regulator involved in nitrogen metabolite repression through the post-translational modulation of AreA, a GATA-type transcription factor in *Aspergillus nidulans* (Andrianopoulos et al. 1998). Transcriptional regulators that use cofactors such as NAD$^+$ and NADP$^+$ are noteworthy because they might function as direct sensors of the metabolic state of the cell (Shi 2004). These cofactors are essential molecules in energy metabolism and are also involved in signaling pathways that regulate processes such as gene transcription and apoptosis (Ying 2006). These observations point toward a possible function for HaRxLL441 in modulating host transcriptional regulation. Our subcellular localization studies suggest that HaRxLL441 might shuttle between the cytoplasm and the nucleus. HaRxL22 and members of this protein family possess amino acid motifs that are present one to five times in their predicted protein sequences, overlap with W-Y-L motifs described for *Phytophthora* effectors (Jiang et al. 2008), and may play important structural roles (Boutemy et al. 2011; Yaeno et al. 2011). Remarkably, like some other HaRxL, GFP-tagged HaRxL89 accumulates in the nucleolus (Caillaud et al. 2012), suggesting a role for HaRxL89 in modulating some nucleolar functions such as ribosomal biogenesis, regulation of mitosis, cell-cycle progression or proliferation, or a role in modulating RNA turnover or the generation of regulatory RNAs (Boisvert et al. 2007; Hernandez-Verdun et al. 2010).

As a result of our experiments on the subcellular localization of the five selected effectors, we observed a cleavage that seems to be site specific in fluorescently tagged HaRxLL464 and HaRxL89, because a unique band was observed in the Western blot in addition to the band corresponding to the full-length chimeric protein. Although the fluorescent signal is not informative about the subcellular localization of HaRxLL464, the Western blot is suggestive of a specific processing by a plant protease. For HaRxL89, because we did not observe any change in the subcellular localization pattern between N- and C-terminal fusions (they all localized to the nucleus and the nucleolus), we speculate that the cleavage site resides between the two direct repeats that coincide with a bipartite nuclear localization sequence (NLS), and we interpret our results to mean that the one NLS remaining attached to GFP drives GFP to the nucleus. Further characterization of these HaRxL using biochemical and cell biological approaches will shed additional light on their functions.

MATERIALS AND METHODS

Bacterial strains, plasmids, and media.

The *P. syringae* pv. *tomato lux* strains expressing HaRxL from Emoy2 used in this study were previously described by Fabro and associates (2011). The EDV-HaRxL constructs were propagated in *Escherichia coli* DH5α or DH10B (Life Technologies, Carlsbad, CA, U.S.A.) and transferred by triparental mating into *P. syringae* pv. *tomato lux* (Fan et al. 2008), *P. syringae* pv. *tomato* ΔCEL (Badel et al. 2003), *P. syringae* pv. *tomato hrcC* (Yuan and He 1996), or *P. fluorescens* EtHan (Thomas et al. 2009). *E. coli* cells were grown in Luria-Bertani (LB) medium (Sambrook et al. 1989) at 37°C and *Pseudomonas* cells were grown in King's B (KB) medium (King et al. 1954) at 28°C.

Plant materials and growth.

Arabidopsis accessions were either obtained from the Nottingham Arabidopsis Stock Centre or provided by P. Kover, University of Bath, U.K. Plants were grown in Scotts and Levington F1 modular compost in controlled environment rooms under short day cycles (10 and 14 h day and night, respectively, and 150 to 200 $\mu E/m^2s$) at 22°C and 60% relative humidity and watered every day from below.

Inoculum preparation and plant inoculations.

For IPECA, suspensions of individual *P. syringae* pv. *tomato* strains were prepared in 10 mM $MgCl_2$ and strains were mixed in equal proportions, pelleted, and then resuspended to the desired final concentration. Leaves of 4- to 5-week-old plants were infiltrated with 1×10^4 CFU/ml using a needleless syringe. Aliquots of the *P. syringae* pv. *tomato* inoculum were stored at –80°C to serve as the input sample. Infected leaves collected at 3 dpi served as the output sample. For in planta growth assays, leaves of 4- to 5-week-old plants were inoculated with 5×10^5 CFU/ml and bacteria counted at 3 dpi as previously described (Glazebrook and Ausubel 1994). Three completely independent experiments with at least three biological repetitions were conducted. For HR elicitation, *P. syringae* pv. *tomato* cell suspensions at an optical density at 600 nm (OD_{600}) = 0.2, 0.02, and 0.002 were infiltrated into *Arabidopsis* leaves. For HR elicitation using *P. fluorescens* EtHAn, assays were conducted essentially as described by Thomas and associates (2009). At least three completely independent experiments infiltrating 24 leaves of each *Arabidopsis* accession with a particular *P. syringae* pv. *tomato* or *P. fluorescens* EtHAn strain were conducted.

Sample preparation and HaRxL detection.

For IPECA-RENSOL, plasmid DNA was isolated from input and output samples according to Llop and associates (1999) and the HaRxL inserts amplified and biotin tagged by PCR with 20 cycles of 95°C for 20 s, 66°C for 30 s, and 72°C for 3.5 min using primers MPF1 and 5'-biotin-MPR2 (Supplementary Table S5). The biotinylated HaRxL were bound to streptavidin beads (Promega Corp., Madison, WI, U.S.A.), washed three times with 0.1× SSC (1× SSC is 0.15 M NaCl plus 0.015 M sodium citrate), and digested with *Aci*I (New England Biolabs, Ipswich, MA, U.S.A.) for 1.5 h at 37°C. The beads were again washed three times with 0.1× SSC, resuspended in a 200 µl of ligation reaction containing 5 U of T4 DNA ligase and 10 pmol of annealed adapter I, and incubated at 20°C for 3 h. The beads were washed three times with 0.1× SSC, and the adapter I-HaRxL fragments were released from the beads by digestion with *Mme*I and precipitated overnight at –20°C. The pelleted adapter I-HaRxL fragments were resuspended in a 20-µl reaction containing 1 U of T4 DNA ligase and 10 pmol annealed adapter II and incubated at 20°C for 3 h. Adapter I-HaRxL fragment-adapter II constructs were amplified using the Phusion PCR kit (Finnzymes, Espoo, Finland) and primers GenX1 and GenX2 with 20 cycles of 98°C for 20 s, 65°C for 30 s, and 72°C for 15 s. The PCR products were purified from a 8% polyacrylamide gel, diluted to 10 nM in 0.1% Tween-20, and sequenced with a Solexa/Illumina GA-1 Genome Analyzer (Illumina, San Diego, CA, U.S.A.) using primer ADPT_GenX_seq1.

For IPECA-RENCAP, leaf samples were ground in 10 mM $MgCl_2$ and serial dilutions were plated on KB solid medium containing antibiotic selection. Tiny bacterial colonies (2,000 to 5,000 CFU/plate) were recovered from the plates after 2 days by washing with 10 mM $MgCl_2$. Plasmid DNA was isolated from input and output samples by alkaline lysis using the Qiagen spin miniprep kit (Qiagen, Valencia, CA, U.S.A.) and the HaRxL inserts were amplified using primers MPF1 and 5′-6-FAM-MPR2 with *Taq* polymerase and 30 cycles of 95°C for 2 min, 95°C for 30 s, 66°C for 30s, and 72°C for 2 min by emulsion PCR (Williams et al. 2006). The 5′-6-FAM-labeled amplicons were digested during 4 h with 5 U each of *Alw*NI, *Xma*I, and *Pml*I in a total volume of 15 µl, and then, subjected to capillary electrophoresis in an Applied Biosystems 3730xl apparatus.

Quantification of HaRXL and calculation of the O/I ratio.

For IPECA-RENSOL, tags were sorted into sample groups based on their barcode sequences and aligned against the HaRxL reference sequences using the matching algorithm SSAHA (Ning et al. 2001). Total tag matches per HaRxL in each sample were tallied and then normalized by dividing by the number of all HaRxL tag matches in that sample to obtain *fi* (frequency of an HaRxL in the input sample) and *fo* (frequency of an HaRxL in the output sample). Changes in HaRxL tag counts were represented as the O/I ratio = *fo/fi*. For IPECA-RENCAP, data were obtained with collection software v3.0. The abundance of each HaRxL in the sample was estimated as the area under each peak in the electropherogram using GeneMapper v4.0, then normalized by dividing by the total area of all HaRxL to obtain the *fi* and *fo* values. The O/I ratio was then calculated as indicated for IPECA-RENSOL.

Bacterial growth in axenic culture.

For growth in liquid medium, 100 µl of a bacterial suspension at OD_{600} = 0.1 in 10 mM $MgCl_2$ was inoculated into 10 ml of KB amended with appropriate antibiotics, the culture was incubated at 28°C with shaking at 220 rpm, and absorbance was measured at different times. For growth on solid medium,

serial dilutions of the bacterial suspensions at OD_{600} = 0.1 were prepared with 10 mM $MgCl_2$, 20 µl were spotted onto solid KB amended with appropriate antibiotics, and the plates were incubated at 28°C. The luminescence of each spot was measured 56 h later using a Photek camera and the number of CFU was counted.

PTI suppression assays.

For suppression of PTI elicited by *P. fluorescens* EtHan in *N. benthamiana*, bacterial suspensions at OD_{600} = 0.2 in 10 mM $MgCl_2$ were infiltrated into fully expanded leaves of *N. benthamiana* using a needleless syringe. PTI was allowed to develop during 7 h, after which a *P. syringae* pv. *tomato* DC3000 suspension at OD_{600} = 0.02 was infiltrated into an overlapping area. Tissue collapse in the overlapping area was evaluated at 3 days postinfiltration and leaves were stained with Trypan blue. Suppression of callose deposition elicited by *P. syringae* pv. *tomato* ΔCEL in *Arabidopsis* was conducted essentially as described by Fabro and associates (2011).

Subcellular localization in *N. benthamiana*.

Agrobacterium tumefaciens GV3101(pMP90) cells expressing HaRxL as N- or C-terminal fusions with GFP in pK7WGF2 or pK7FWG2, respectively, or N- or C-terminal fusions with RFP in pH7WGR2 or pB7RWG2, respectively (University of Gent Gateway vectors), were grown overnight in liquid LB medium containing appropriate antibiotics. Cells were washed once with 10 mM morpholineethanesulfonic acid (pH 5.6) and 10 mM $MgCl_2$ and resuspended at OD_{600} = 0.2. Acetosyringone was added to a final concentration of 200 µM and incubated with shaking for 2 h. Leaves of 3- to 4-week-old *N. benthamiana* were syringe infiltrated and fluorescence was observed after 2 days in a Leica DM6000B/TCS SP5 confocal microscope (Leica Microsystems, Milton Keynes, U.K.) with laser excitation for GFP at 488 nm and for RFP at 561 nm. At least three independent constructs of both GFP and RFP fusions to the C and N terminus of each effector were tested, with similar results. Plasmolysis experiments were performed by syringe-infiltration of 2 M sucrose into leaf samples expressing GFP-tagged HaRxL75. Pictures were taken 5 to 15 min after sucrose treatment.

Protein extractions and analyses.

Immunoblot analyses were performed on protein extracts prepared by grinding leaf samples in liquid nitrogen and resuspending in extraction buffer (5% [vol/vol] glycerol, 150 mM Tris [pH 7.5], 5 mM EDTA, 150 mM NaCl, 1% [vol/vol] Triton X-100, 10 mM dithiothreitol, 2% [wt/vol] polyvinylpolypyrrolidone, and 1× protease inhibitor cocktail [Sigma-Aldrich, St. Louis]). Protein extracts were mixed and spun at full speed (16,000 × *g*) at 4°C, and supernatants were separated from pellets. Samples were loaded onto and separated in standard sodium dodecyl sulfate polyacrylamide gel electrophoresis gels (10% acrylamide) and blotted using standard procedures. Blots were blocked at room temperature using Tris-buffered saline (TBS)-Tween 20 (TBST)-milk (5% wt/vol) for 1 h and then the α-GFP antibody (Roche) was added to the TBST-milk (1:3,000, 5%) for 1 h. Blots were washed three times in TBST for 10 min before being probed with HRP-conjugated α-rabbit polyclonal antibody (Sigma-Aldrich). Blots were washed three times in TBST followed by three times in TBS before being developed using the Pierce horseradish peroxidase detection kit (Thermo Scientific, Sugarland, TX, U.S.A.) and exposed for 5 min.

Effector expression during Emoy2 infection.

Four-week-old *Arabidopsis thaliana* Ws *eds1-1* plants were spray inoculated with Emoy2 at 5 × 10^4 spores/ml, and 20 leaves from five different plants were collected at 0, 12, 24, 48, 72, and 168 h postinoculation. Total RNA was extracted using the TRI-REAGENT (Sigma-Aldrich). cDNA was synthesized from 2 µg of high-quality RNA with the oligo dT 3′ primer CDSIII/3′ (SMART Technology, Clontech, CA, U.S.A.). Internal fragments of the effectors were amplified from cDNA at 10 ng/µl using high-fidelity Phusion polymerase (Finnzymes) and gene-specific primers, and amplicons were sequenced.

ACKNOWLEDGMENTS

We thank the horticulturist team at the John Innes Centre for growing plants; D. Baker (The Genome Analysis Center, Norwich, U.K.) for assistance on capillary electrophoresis; P. Kover (University of Bath) for providing seed of the "MAGIC" founders; L. Wirthmueller (The Sainsbury Laboratory) for comments on the manuscript; and J. Dangl, D. Weigel, and M. Doebeli for useful discussions. Prohibited plant pathogens are held under license from FERA; PHSI 713/6755 (04/2012). This work was supported by grants HFSP RGP0057/20067-C to D. Greenshields, J. L. Badel, and J. D. G. Jones; BBSRC ERA-PG Effectoromics, Deutsche Forschungsgemeinshaft JEP/DFG, and NGI/NOW to G. Fabro and J. D. G. Jones; Gatsby Foundation GAT2545 to S. J. M. Piquerez and G. Fabro; BBSRC BB/F0161901 and BB/E024882/1 to N. Ishaque and J. D. G. Jones; BBSRC CASE studentship T12144 to N. Ishaque; and Marie Curie early stage training program fellowship 019727 to S. J. M. Piquerez. J. D. G. Jones, J. L. Badel, and D. Greenshields conceived and designed the experiments; J. L. Badel and G. Fabro performed the PTI assays; J. L. Badel, D. Greenshields, and S. J. M. Piquerez performed the pathotests; J. L. Badel and S. J. M. Piquerez performed the subcellular localization; J. L. Badel, D. Greenshields, and G. Rallapalli performed the IPECA assays; J. L. Badel and N. Ishaque provided bioinformatics; J. L. Badel and G. Fabro provided effector expression during Emoy2 infection; J. L. Badel provided in vitro bacterial growth assays; J. L. Badel, D. Greenshields, and G. Rallapalli analyzed the data; J. L. Badel wrote the article; and J. D. G. Jones, G. Fabro, and S. J. M. Piquerez edited the article.

LITERATURE CITED

Abramovitch, R. B., Kim, Y.-J., Chen, S., Dickman, M. B., and Martin, G. B. 2003. *Pseudomonas* type III effector AvrPtoB induces plant disease susceptibility by inhibition of host programmed cell death. EMBO (Eur. Mol. Biol. Organ.) J. 22:60-609.

Allen, R. L., Bittner-Eddy, P. D., Grenville-Briggs, L. J., Meitz, J. C., Rehmany, A. P., Rose, L. E., and Beynon, J. L. 2004. Host-parasite coevolutionary conflict between *Arabidopsis* and downy mildew. Science 306:1957-1960.

Andrianopoulos, A., Kourambas, S., Sharp, J. A., Davis, M. A., and Hynes, M. J. 1998. Characterization of the *Aspergillus nidulans* nmrA gene involved in nitrogen metabolite repression. J. Bacteriol. 180:1973-1977.

Badel, J. L., Charkowski, A. O., Deng, W.-L., and Collmer, A. 2002. A gene in the *Pseudomonas syringae* pv. *tomato* Hrp pathogenicity island conserved effector locus, *hopPtoA1*, contributes to efficient formation of bacterial colonies in planta and is duplicated elsewhere in the genome. Mol. Plant-Microbe Interact. 15:1014-1024.

Badel, J. L., Nomura, K., Bandyopadhyay, S., Shimizu, R., Collmer, A., and He, S. Y. 2003. *Pseudomonas syringae* pv. *tomato* DC3000 HopPtoM (CEL ORF3) is important for lesion formation but not growth in tomato and is secreted and translocated by the Hrp type III secretion system in a chaperone-dependent manner. Mol. Microbiol. 49:1239-1251.

Badel, J. L., Shimizu, R., Oh, H. S., and Collmer, A. 2006. A *Pseudomonas syringae* pv. tomato *avrE1/hopM1* mutant is severely reduced in growth and lesion formation in tomato. Mol. Plant-Microbe Interact. 19:99-111.

Bailey, K., Cevik, V., Holton, N. J., Byrne-Richardson, J., Sohn, K. H., Coates, M., Woods-Tör, A., Aksoy, H. M., Hughes, L., Baxter, L., Jones, J. D. G., Benyon, J. Holub, E. B., and Tör, M. 2011. Molecular cloning of *ATR5*Emoy2 from *Hyaloperonospora arabidopsidis*, an avirulence determinant that triggers *RPP5*-mediated defense in *Arabidopsis*. Mol. Plant-Microbe Interact. 24:827-838.

Baxter, L., Tripathy, S., Ishaque, N., Boot, N., Cabral, A., Kemen, E., Thines, M., Ah-Fong, A., Anderson, R., Badejoko, W., Bittner-Eddy, P., Boore, J. L., Chibucos, M. C., Coates, M., Dehal, P., Delehaunty, K., Dong, S., Downton, P., Dumas, B., Fabro, G., Fronick, C., Fuerstenberg, S. I., Fulton, L., Gaulin, E., Govers, F., Hughes, L., Humphray, S., Jiang, R. H., Judelson, H., Kamoun, S., Kyung, K., Meijer, H., Minx, P., Morris,

P., Nelson, J., Phuntumart, V., Qutob, D., Rehmany, A., Rougon-Cardoso, A., Ryden, P., Torto-Alalibo, T., Studholme, D., Wang, Y., Win, J., Wood, J., Clifton, S. W., Rogers, J., Van den Ackerveken, G., Jones, J. D., McDowell, J. M., Beynon, J., and Tyler, B. M. 2010. Signatures of adaptation to obligate biotrophy in the *Hyaloperonospora arabidopsidis* genome. Science 330:1549-1551.

Benjamini, Y., and Hochberg, Y. 1995. Controlling the false discovery rate: A practical and powerful approach to multiple testing. J. R. Stat. Soc. B, 57:289-300.

Beuzon, C. R., and Holden, D. W. 2001. Use of mixed infections with *Salmonella* strains to study virulence genes and their interactions *in vivo*. Microbes Infect. 3:1345-1352.

Bhattacharjee, S., Hiller, N.L., Liolios, K., Win, J., Kanneganti, T. D., Young, C., Kamoun, S., and Haldar, K. 2006. The malarial host-targeting signal is conserved in the Irish potato famine pathogen. PLoS Pathog. 2:453-465. Published online.

Birch, P. R. J., Rehmany, A. P., Pritchard, L., Kamoun, S., and Beynon, J. L. 2006. Trafficking arms: Oomycete effectors enter host plant cells. Trends Microbiol. 14:8-11.

Boisvert, F. M., van Koningsbruggen, S., Navascues, J., and Lamond, A. I. 2007. The multifunctional nucleolus. Nat. Rev. Mol. Cell. Biol. 8:574-585.

Boutemy, L. S., King, S. R., Win, J., Hughes, R. K., Clarke, T. A., Blumenschein, T. M., Kamoun, S., and Banfield, M. J. 2011. Structures of *Phytophthora* RXLR effector proteins: A conserved but adaptable fold underpins functional diversity. J. Biol. Chem. 286:35834-42.

Brooks, D. M., Hernández-Guzmán, G., Kloek, A. P., Alarcón-Chaidez, F., Sreedharan, A., Rangaswamy, V., Peñaloza-Vázquez, A., Bender, C. L., and Kunkel, B. N. 2004. Identification and characterization of a well-defined series of coronatine biosynthetic mutants of *Pseudomonas syringae* pv. *tomato* DC3000. Mol. Plant-Microbe Interact. 17:162-174.

Cabral, A., Stassen, J. H., Seidl, M. F., Bautor, J., Parker, J. E., and Van den Ackerveken, G. 2011. Identification of *Hyaloperonospora arabidopsidis* transcript sequences expressed during infection reveals isolate-specific effectors. PLoS One 6:e19328. Published online.

Caillaud, M.-C., Fabro, G., Steinbrenner, J., Ishaque, N., Beynon, J., and Jones, J. D. G. 2012. Subcellular localization of the *Hpa* RxLR effector repertoire identifies the extrahaustorial membrane-localized HaRxL17 that confers enhanced plant susceptibility. Plant J. 69:252-265.

Chaparro-Garcia, A., Wilkinson, R. C., Gimenez-Ibanez, S., Findlay, K., Coffey, M. D., Zipfel, C., Rathjen, J. P., Kamoun, S., and Schornack, S. 2011. The receptor-like kinase SERK3/BAK1 is required for basal resistance against the late blight pathogen *Phytophthora infestans* in *Nicotiana benthamiana*. PLoS One 6:e16608. Published online.

Crabill, E., Joe, A., Block, A., van Rooyen, J. M., and Alfano, J. R. 2010. Plant immunity directly or indirectly restricts the injection of type III effectors by the *Pseudomonas syringae* type III secretion system. Plant Physiol. 154:233-244.

DebRoy, S., Thilmony, R., Kwack, Y. B., Nomura, K., and He, S. Y. 2004. A family of conserved bacterial effectors inhibits salicylic acid-mediated basal immunity and promotes disease necrosis in plants. Proc. Natl. Acad. Sci. U.S.A. 101:9927-9932.

Dou, D., Kale, S. D., Wang, X., Chen, Y., Wang, Q., Jiang, R. H., Arredondo, F. D., Anderson, R. G., Thakur, P. B., McDowell, J. M., Wang, Y., and Tyler, B. M. 2008a. Conserved C-terminal motifs required for avirulence and suppression of cell death by *Phytophthora sojae* effector Avr1b. Plant Cell 20:1118-1133.

Dou, D., Kale, S. D., Wang, X., Jiang, R. H., Bruce, N. A., Arredondo, F. D., Zhang, X., and Tyler, B. M. 2008b. RXLR-mediated entry of *Phytophthora sojae* effector Avr1b into soybean cells does not require pathogen-encoded machinery. Plant Cell 20:1930-1947.

Fabro, G., Steinbrenner, J., Coates, M., Ishaque, N., Baxter, L., Studholme, D., Köerner, E., Allen, R., Piquerez, S. J. M., Rougon-Cardoso, A., Greenshields, D., Lei, R., Badel, J. L., Caillaud, M.-C., Van den Ackerveken, G., Parker, J. E., Beynon, J., and Jones, J. D. G. 2011. The effectorome from the obligate biotroph *Hyaloperonospora arabidopsidis* reveals redundant roles in suppression of PAMP-Triggered Immune response. PLoS Pathog. 7:e1002348. Published online.

Fan, J., Crooks, C., and Lamb, C. 2008. High-throughput quantitative luminescence assay of the growth in planta of *Pseudomonas syringae* chromosomally tagged with *Photorhabdus luminescens luxCDABE*. Plant J. 53:393-399.

Gassmann, W., Hinsch, M. E., and Staskawicz, B. J. 1999. The *Arabidopsis RPS4* bacterial-resistance gene is a member of the TIR-NBS-LRR family of disease-resistance genes. Plant J. 20:265-277.

Gimenez-Ibanez, S., Hann, D. R., Ntoukakis, V., Petutschnig, E., Lipka, V., and Rathjen, J. P. 2009. AvrPtoB targets the LysM receptor kinase CERK1 to promote bacterial virulence on plants. Curr. Biol. 19:423-429.

Glazebrook, J., and Ausubel, F. M. 1994. Isolation of phytoalexin-deficient mutants of *Arabidopsis thaliana* and characterization of their interactions with bacterial pathogens. Proc. Natl. Acad. Sci. U.S.A. 91:8955-8959.

Gohre, V., and Robatzek, S. 2008. Breaking the barriers: Microbial effector molecules subvert plant immunity. Annu. Rev. Phytopathol. 46:189-215.

Goritschnig, S., Krasileva, K. V., Dahlbeck, D., and Staskawicz, B. J. 2012. Computational prediction and molecular characterization of an oomycete effector and the cognate *Arabidopsis* resistance gene. PLoS Genet. 8:e1002502. Published online.

Grouffaud, S., van West, P., Avrova, A. O., Birch, P. R., and Whisson, S. C. 2008. *Plasmodium falciparum* and *Hyaloperonospora parasitica* effector translocation motifs are functional in *Phytophthora infestans*. Microbiology 154:3743-3751.

Guo, M., Tian, F., Wamboldt, Y., and Alfano, J. R. 2009. The majority of the type III effector inventory of *Pseudomonas syringae* pv. *tomato* DC3000 can suppress plant immunity. Mol. Plant-Microbe Interact. 22:1069-1080.

Hann, D. R., and Rathjen, J. P. 2007. Early events in the pathogenicity of *Pseudomonas syringae* on *Nicotiana benthamiana*. Plant J. 49:607-618.

Hauck, P., Thilmony, R., and He, S. Y. 2003. A *Pseudomonas syringae* type III effector suppresses cell wall-based extracellular defense in susceptible *Arabidopsis* plants. Proc. Natl. Acad. Sci. U.S.A. 100:8577-8582.

Hernandez-Verdun, D., Roussel, P., Thiry, M., Sirri, V., and Lafontaine, D. L. J. 2010. The nucleolus: Structure/function relationship in RNA metabolism. Wiley Interdisciplinary Rev. 1:415-431.

Holub, E. B. 2006. Evolution of parasitic symbioses between plants and filamentous microorganisms. Curr. Opin. Plant Biol. 9:397-405.

Holub, E. B. 2008. Natural history of *Arabidopsis thaliana* and oomycete symbioses. Eur. J. Plant. Pathol. 122:91-109.

Jiang, R. H. Y., Tripathy, S., Govers, F., and Tyler, B. M. 2008. RXLR effector reservoir in two *Phytophthora* species is dominated by a single rapidly evolving superfamily with more than 700 members. Proc. Natl. Acad. Sci. U.S.A. 105:4874-4879.

Jones, J. D., and Dangl, J. L. 2006. The plant immune system. Nature 444:323-329.

Kelley, B. S., Lee, S. J., Damasceno, C. M., Chakravarthy, S., Kim, B. D., Martin, G. B., and Rose, J. K. 2010. A secreted effector protein (SNE1) from *Phytophthora infestans* is a broadly acting suppressor of programmed cell death. Plant J. 62:357-366.

King, E. O., Ward, M. K., and Raney, D. E. 1954. Two simple media for the demonstration of pyocyanin and fluorescin. J. Lab. Clin. Med. 44:301-330.

Klement, Z., and Goodman, R. N. 1967. The hypersensitive reaction to infection by bacterial plant pathogens. Annu. Rev. Phytopathol. 5:17-44.

Kover, P. X., Valdar, W., Trakalo, J., Scarcelli, N., Ehrenreich, I. M., Purugganan, M. D., Durrant, C., and Mott, R. 2009. A multiparent advanced generation inter-cross to fine-map quantitative traits in *Arabidopsis thaliana*. PLoS Genet. 5:e1000551. Published online.

Llop, P., Caruso, P., Cubero, J., Morente, C., and Lopez, M. M. 1999. A simple extraction procedure for efficient routine detection of pathogenic bacteria in plant material by polymerase chain reaction. J. Microbiol. Methods 37:23-31.

Macho, A. P., Zumaquero, A., Ortiz-Martin, I., and Beuzon, C. R. 2007. Competitive index in mixed infections: A sensitive and accurate assay for the genetic analysis of *Pseudomonas syringae*-plant interactions. Mol. Plant Pathol. 8:437-450.

Mansfield, J. W. 2009. From bacterial avirulence genes to effector functions via the *hrp* delivery system: An overview of 25 years of progress in our understanding of plant innate immunity. Mol. Plant Pathol. 10:721-734.

Melotto, M., Underwood, W., Koczan, J., Nomura, K., and He, S. Y. 2006. Plant stomata function in innate immunity against bacterial invasion. Cell 126:969-980.

Mittal, S., and Davis, K. R. 1995. Role of the phytotoxin coronatine in the infection of *Arabidopsis thaliana* by *Pseudomonas syringae* pv. *tomato*. Mol. Plant-Microbe Interact. 8:165-171.

Munkvold, K. R., Russell, A. B., Kvitko, B. H., and Collmer, A. 2009. *Pseudomonas syringae* pv. *tomato* DC3000 Type III effector HopAA1-1 functions redundantly with chlorosis-promoting factor PSPTO4723 to produce bacterial speck lesions in host tomato. Mol. Plant-Microbe Interact. 11:1341-1355.

Nguyen, H. P., Chakravarthy, S., Velasquez, A. C., McLane, H. L., Zeng, L., Nakayashiki, H., Park, D. H., Collmer, A., and Martin, G. B. 2010. Methods to study PAMP-triggered immunity using tomato and *Nicotiana benthamiana*. Mol. Plant-Microbe Interact. 23:991-999.

Ning, Z., Cox, A. J., and Mullikin, J. C. 2001. SSAHA: A fast search method for large DNA databases. Genome Res. 11:1725-1729.

Oh, H. S., and Collmer, A. 2005. Basal resistance against bacteria in *Nicotiana benthamiana* leaves is accompanied by reduced vascular staining

and suppressed by multiple *Pseudomonas syringae* type III secretion system effector proteins. Plant J. 44:348-359.

Oh, H. S., Park, D. H., and Collmer, A. 2010. Components of the *Pseudomonas syringae* type III secretion system can suppress and may elicit plant innate immunity. Mol. Plant-Microbe Interact. 23:727-739.

Oh, S. K., Young, C., Lee, M., Oliva, R., Bozkurt, T. O., Cano, L. M., Win, J., Bos, J. I., Liu, H. Y., van Damme, M., Morgan, W., Choi, D., Van der Vossen, E. A. G., Vleeshouwers, V., and Kamoun, S. 2009. In planta expression screens of *Phytophthora infestans* RXLR effectors reveal diverse phenotypes, including activation of the *Solanum bulbocastanum* disease resistance protein Rpi-blb2. Plant Cell 21:2928-2947.

Rehmany, A. P., Gordon, A., Rose, L. E., Allen, R. L., Armstrong, M. R., Whisson, S. C., Kamoun, S., Tyler, B. M., Birch, P. R., and Beynon, J. L. 2005. Differential recognition of highly divergent downy mildew avirulence gene alleles by *RPP1* resistance genes from two *Arabidopsis* lines. Plant Cell 17:1839-1850.

Rossmann, M. G., Moras, D., and Olsen, K. W. 1974. Chemical and biological evolution of nucleotide-binding protein. Nature 250:194-199.

Sambrook, J., Fritsch, E. F., and Maniatis, T. 1989. Molecular Cloning: A Laboratory Manual. Cold Spring Harbor Laboratory Press, Cold Spring Harbor, NY, U.S.A.

Shi, Y. 2004. Metabolic enzymes and coenzymes in transcription—A direct link between metabolism and transcription? Trends Genet. 20:445-452.

Sohn, K. H., Lei, R., Nemri, A., and Jones, J. D. G. 2007. The downy mildew effector proteins ATR1 and ATR13 promote disease susceptibility in *Arabidopsis thaliana*. Plant Cell 19:4077-4090.

Sohn, K. H., Zhang, Y., and Jones, J. D. 2009. The *Pseudomonas syringae* effector protein, AvrRPS4, requires in planta processing and the KRVY domain to function. Plant J. 57:1079-1091.

Thomas, W. J., Thireault, C. A., Kimbrel, J. A., and Chang, J. H. 2009. Recombineering and stable integration of the *Pseudomonas syringae* pv. *syringae* 61 *hrp/hrc* cluster into the genome of the soil bacterium *Pseudomonas fluorescens* Pf0-1. Plant J. 60:919-928.

Underwood, W., Zhang, S. Q., and He, S. Y. 2007. The *Pseudomonas syringae* type III effector tyrosine phosphatase HopAO1 suppresses innate immunity in *Arabidopsis thaliana*. Plant J. 52:658-672.

Whisson, S. C., Boevink, P. C., Moleleki, L., Avrova, A. O., Morales, J. G., Gilroy, E. M., Armstrong, M. R., Grouffaud, S., van West, P., Chapman, S., Hein, I., Toth, I. K., Pritchard, L. and Birch, P. R. J. 2007. A translocation signal for delivery of oomycete effector proteins into host plant cells. Nature 450:115-118.

Williams, R., Peisajovich, S. G., Miller, O. J., Magdassi, S., Tawfik, D. S., and Griffiths, A. D. 2006. Amplification of complex gene libraries by emulsion PCR. Nat. Methods 3:545-550.

Willmann, R., Lajunen, H. M., Erbs, G., Newman, M.-A., Kolb, D., Tsuda, K., Katagiri, F., Fliegmann, J., Bono, J.-J., Cullimore, J. V., Jehle, A. K., Götz, F., Kulik, A., Molinaro, A., Lipka, V., Gust, A. A., and Nürnberger, T. 2011. *Arabidopsis* lysin-motif proteins LYM1 LYM3 CERK1 mediate bacterial peptidoglycan sensing and immunity to bacterial infection. Proc. Natl. Acad. Sci. U.S.A. 108:19824-19829.

Win, J., Morgan, W., Bos, J., Krasileva, K. V., Cano, L. M., Chaparro-Garcia, A., Ammar, R., Staskawicz, B. J., and Kamoun, S. 2007. Adaptive evolution has targeted the C-terminal domain of the RXLR effectors of plant pathogenic oomycetes. Plant Cell 19:2349-2369.

Yaeno, T., Li, H., Chaparro-Garcia, A., Schornack, S., Koshiba, S., Watanabe, S., Kigawa, T., Kamoun, S., and Shirasu, K. 2011. Phosphatidylinositol monophosphate-binding interface in the oomycete RXLR effector AVR3a is required for its stability in host cells to modulate plant immunity. Proc. Natl. Acad. Sci. U.S.A. 108:14682-14687.

Ying, W. 2006. NAD^+ and NADH in cellular functions and cell death. Front. Biosci. 11:3129-3148.

Yu, I. C., Parker, J., and Bent, A. F. 1998. Gene-for-gene disease resistance without the hypersensitive response in *Arabidopsis dnd1* mutant. Proc. Natl. Acad. Sci. U.S.A. 95:7819-7824.

Yuan, J., and He, S. Y. 1996. The *Pseudomonas syringae* Hrp regulation and secretion system controls the production and secretion of multiple extracellular proteins. J. Bacteriol. 178:6399-6402.

Zhang, J., and Zhou, J. M. 2010. Plant immunity triggered by microbial molecular signatures. Mol. Plant 3:783-793.

Zhang, J., Shao, F., Li, Y., Cui, H., Chen, L., Li, H., Zou, Y., Long, C., Lan, L., Chai, J., Chen, S., Tang, X., and Zhou, J. M. 2007. A *Pseudomonas syringae* effector inactivates MAPKs to suppress PAMP-induced immunity in plants. Cell Host Microbe 1:175-185.

Zipfel, C., and Robatzek, S. 2010. Pathogen-associated molecular pattern-triggered immunity: Veni: vidi…? Plant Physiol. 154:551-554.